

Impact Analysis Of Wildfire By Means Of Satellite Based Cyber-Physical System

Nasru Minallah, M. Nouman Khan , Waleed Khan, Muhammad Athar Javed Sethi, Atif Sardar Khan

Abstract: This work proposes a satellite based Cyber-Physical System for impact analysis of wildfire. Wildfire can may occur due to human activities or natural phenomenon such as lightning and have substantial impact on living beings and the environment. Analysis of Australia wildfire shows a drastic change in vegetation and atmosphere of Australia. Biomass burning is one of major source of emission of pollutants. The major air pollutants are carbon dioxide (CO_2), carbon monoxide (CO), nitrogen dioxide (NO_2), ozone (O_3), sulfur dioxide (SO_2), formaldehyde ($HCHO$) and particulate matter (PM). To monitor air quality, we have to investigate the extent of these gases in air. Traditional method involving installation of embedded systems-based air quality measurement equipment are too much costly and have limitations as it can be installed in a limited area. Satellite-based Cyber-Physical System is an alternate technique for detecting damages caused by wildfire. This paper aims to investigate impact of wildfire on atmosphere and vegetation of Australia, through Satellite-based Cyber-Physical System, while employing Sentinel-5 Precursor (Sentinel-5p) and Landsat 8 satellites using Google Earth Engine. Using our proposed Cyber-Physical System, we processed pre-fire dataset (2019-11-05 -to- 2019-11-07) and post-fire dataset (2019-11-08 -to- 2019-11-13) of Sentinel-5p and Landsat 8 in utilizing Google Earth Engine. Our analysis shows a severe decrease, of nearly 100%, in healthy vegetation and drastic increase of almost 112% in NO_2 , 260% in CO , 264% in aerosol index, 144% in $HCHO$ in New South Wales and its nearby cities of Australia. Our analysis proved that as compared to up-to-date fire monitoring systems, our proposed Satellite-based Cyber-Physical System have a great potential in making critical decisions and shows appreciable performance in productivity, safety, reliability and serviceability.

Index Terms: Wildfire; environment; Atmosphere; Pollutants; Google Earth Engine; Sentinel-5p, Landsat 8;

1 INTRODUCTION

ON November 8th of 2019, a drastic fire was reported in New South Wales(NSW) [1], which is southeastern Australian state. Australia had wildfire since ages but this time damages were severe than usual. Approximately 27 people, countless animals were died, 2,000 homes were damaged by the wildfire and more than 12.35 million acres (equivalent to the size of South Korea) have been burned [2]. A total of \$110 billion economic loss due to this wildfire was estimated [3]. Wildfire can be ignited sometimes by human activities (anthropogenic) but mostly by natural phenomenon such as lightning striking dry vegetation. Millions of hectors forest is burnt yearly and Millions of dollars are spent on its recovery by Australian government [4]. As wildfire counts in anthropogenic process and has been a detriment to environment. Figure 1

Reference source not found. shows that wildfire accelerates the production of;

- Harmful pollution like carbon monoxide (CO), formaldehyde ($HCHO$), Nitrogen dioxide (NO_2) and ozone(O_3)
 - Particulate pollutants like dust, fume, mist and smoke
- Other health and environmental hazards like acid rain, the

greenhouse effect, depletion of ozone layer and deforestation.

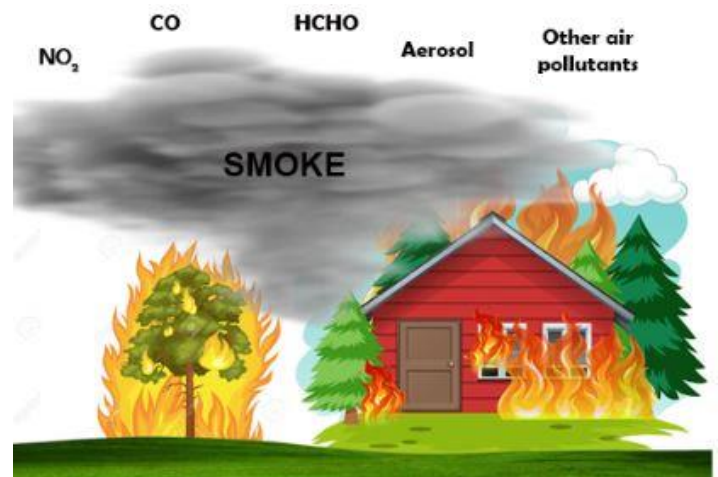


Fig. 1. Effect of forest fire on atmosphere

Cyber-Physical System(CPS) is actually joint collaboration of computing and physical components systems. CPS brought advances in emerging fields like forest fire monitoring, personalized health care and traffic flow management [5]. The core of cyber-physical systems is computing elements and sensors that monitor preset cyber-physical indicators and send data to the system's next level. Depending on this data input, different control decisions are taken and the executive elements in the system make changes in the environment that can lower the risk of emergencies [6]. The advantages of using CPS in forest-fire monitoring are as follows[7]:

- Higher efficiency of the procedures of monitoring, control and administration of geographically distributed regions, due to real-time data exchange between the system levels;
- Prompt scaling and transport of any level of the system in space;
- Higher reliability of data about the environment and about potentially hazardous objects.

- The work has been carried out under the umbrella of National Center for Big data and Cloud Computing (NCBC), University of Engineering and Technology, Peshawar, Pakistan
- Corresponding Author: Nasru Minallah, Email: n.minallah@uetpeshawar.edu.pk
- Nasru Minallah is Associate Professor at Department for Computer Systems Engineering (DCSE) at University of Engineering and Technology Peshawar (UET Peshawar), and Principle Investigator of National Center for Big Data and Cloud Computing (NCBC).
- M. Nouman Khan is pursuing his Master Degree in Computer Systems Engineering from DCSE, UET Peshawar and as Research Assistant at NCBC.
- Waleed Khan is currently pursuing his PhD in Computer Systems Engineering from DCSE, UET Peshawar. He is also serving as Research Associate at NCBC.
- Athar Sethi is Assistant Professor at DCSE, UET Peshawar
- Atif Sardar Khan is currently pursuing his PhD from Department of Electrical Engineering, UET Peshawar, and is serving as Lecturer, at the department.

• Higher efficiency of resource administration, due to optimized performance of applications when current changes are considered. Cyber-physical systems have a great potential in making critical decisions, as in comparison to the up-to-date distributed systems, they show higher productivity, safety, reliability and serviceability [8-10]. Forest research using remotely sensed satellite data is one of state of the art application of CPS [11-13]. Satellite data is very effective and useful for forest fire risk assessment as it has very quick response to investigate vegetation status and its impact on environment after forest fire [14]. Traditional methods, like on ground sensor based data collection and monitoring, are also helpful for wildfire risk assessment but these methods are costly, time consuming and have limited applications in remote areas [15]. In comparison with ground based sensors methods, satellite based CPS is one of the emerging method for the assessment of extent of forest wildfire and to estimate, map, and assess forest fire risk in a cost effective and time-efficient manner with high accuracy at local and large scale [16, 17]. By overlying fire risk variables like vegetation indices, topography, meteorology, Land Surface Temperature(LST) in GIS, fire risk maps can be created [18]. In order to detect damages due to wildfire a lot of data can be processed through Google Earth Engine(GEE), which is an effective procedure for forest fire risk assessment as it can evaluate complex data sets at the same scale [19]. To achieve this goal, in the current study we propose development of satellite-based CPS for impact analysis of wildfire. The rest of the paper is organized as follows. Section 2, discusses satellites data and tool used for this work. Our study area is discussed in section 3. Following section 3, section 4 provides detailed results and discussion about the results obtained after processing the study area related data via our proposed satellite-based CPS. The last section, which is conclusion, will summarize our work.

Table 1 Landsat 8 Band, Spatial Resolution and Spectral Range [22]

Band	Spatial Resolution(m)	Spectral Range(μm)
Band 1(Coastal/aerosol)	30	0.43 to 0.45
Band 2(Blue)	30	0.450 to 0.51
Band 3(Green)	30	0.53 to 0.59
Band 4(Red)	30	0.64 to 0.67
Band 5(Near-Infrared)	30	0.85 to 0.88
Band 6(SWIR 1)	30	1.57 to 1.65
Band 7(SWIR 2)	30	2.11 to 2.29
Band 8(Panchromatic)	15	0.50 to 0.68
Band 9(Cirrus)	30	1.36 to 1.38
Band 10(Thermal Infrared1)	100	10.6 to 11.19
Band 11(Thermal Infrared2)	100	11.50 to 12.51

The Copernicus Sentinel-5P satellite, with TROPospheric Monitoring Instrument (TROPOMI) as payload, was successfully launched in October 2017 by European Space Agency(ESA) [20]. The TROPOMI is a spectrometer, which perform measurements in the UV, visible, near-infrared and short-wave infrared band which make capable Sentinel-5P to sense all atmospheric gases like O_3 , NO_2 , HCHO, SO_2 , CO, CH_4 and aerosol aspects like the aerosol index [21].

3. STUDY AREA

Table 2 shows details of the products of Sentinel-5P.

TROPOMI has a full global coverage each day, but with a much improved resolution ($3.5 \times 7 \text{ km}^2$) [22]. Compared to OMI and GOME, the Sentinel-5P observations are expected to be of significant importance for estimating pollutant concentrations and emissions at the scale of smaller towns, individual power plants, wildfires and major infrastructures [23]. In our proposed satellite-based CPS, we processed Sentinel-5P and Landsat 8 datasets while utilizing Google Earth Engine(GEE). GEE is a web portal providing global time-series SRS and vector data, cloud-based computing, and access to software and algorithms for processing such data [24]. GEE can process data of different satellites like complete Landsat series; Moderate Resolution Imaging Spectrometer (MODIS); National Oceanographic and Atmospheric Administration Advanced very high resolution radiometer (NOAA AVHRR), Sentinel 1, 2, and 3 and Advanced Land Observing Satellite (ALOS). Further details are provided by GEE developers in <https://earthengine.google.com/datasets/>. Numerous studies related to the area of deforestation, drought analysis, disaster investigation, disease detection, food security, water management, climate monitoring and environmental protection are carried out using GEE [24].

2. STUDY AREA

In this article, Australia as our study area as shown in Figure 2, which is located on the geographic coordinates of 25.0000° S latitude and 135.0000° E longitude. Australia total land area is $7,682,300 \text{ Km}^2$ having 25.4 million populations and is 55th in pollution. Australian is one of the most fire vulnerable country of the world. Every year wildfires in Australia causes tremendous damage to properties and results in loss of humans and animals.

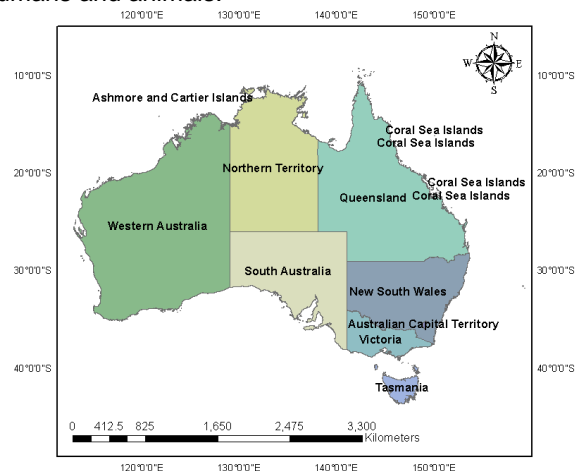


Fig. 2. Study Area

Table 2. Sentinel-5P Data Products, Main Parameters and Spectral Range

S.N0	S5-p Data Product [21]	Main Parameter	Spectral Range(nm) [21]
1	Ozone profiles	Total and tropospheric profiles	270-330
2	Sulphur Dioxide (SO_2)	Total column	308-325
3	Ozone (O_3)	Total column	325-337
4	UV Aerosol Index	aerosol Index	336-440
5	Formaldehyde	Total	337-360

6	(HCHO) Nitrogen Dioxide	column Total column	405-500
7	(NO ₂) Aerosol Layer Height	mid-level pressure	440-460
8	Cloud	Fraction, albedo, top pressure	460-490
10	Methane (CH ₄)	Total column	1590- 1675
11	Carbon monoxide (CO)	Total column	2305- 2385

3. OBSERVATION AND DISCUSSIONS

In our Satellite-based CPS for impact analysis of forest wildfire, we utilize ESA Copernicus remotely sensed data for processing through GEE. Our aim of this study is to detect damage to vegetation and atmosphere in affected cities of Australia due to drastic 2019-20 wildfire using our designed Satellite-based CPS. Flow chart shown in **Error! Reference source not found.** Figure 4 pictorially presents our proposed strategy used in this work.

3.1. IMPACT OF FOREST WILDFIRE ON VEGETATION

In our proposed satellite-based CPS, we processed Landsat 8 remotely sensed pre-fire and post-fire data. Table 3 shows Smoke over affected cities of Australia. In order to detect change in vegetation of the affected cities, we calculated Normalized Difference Vegetation Index (NDVI) for vegetation detection. NDVI essentially gives an indication of the amount of green vegetation in an area. NDVI calculations are based on the idea that green plants (chlorophyll) strongly absorb radiations in the visible band of the electromagnetic spectrum for the photosynthesis process and strongly reflect radiations in the Near Infrared region(NIR) [25].

The NDVI is calculated according to the following formula[26]:

$$NDVI = \frac{(NIR - Red)}{(NIR + Red)} \quad (1)$$

Where

NIR - reflection in the near-infrared spectrum

RED - reflection in the red range of the spectrum

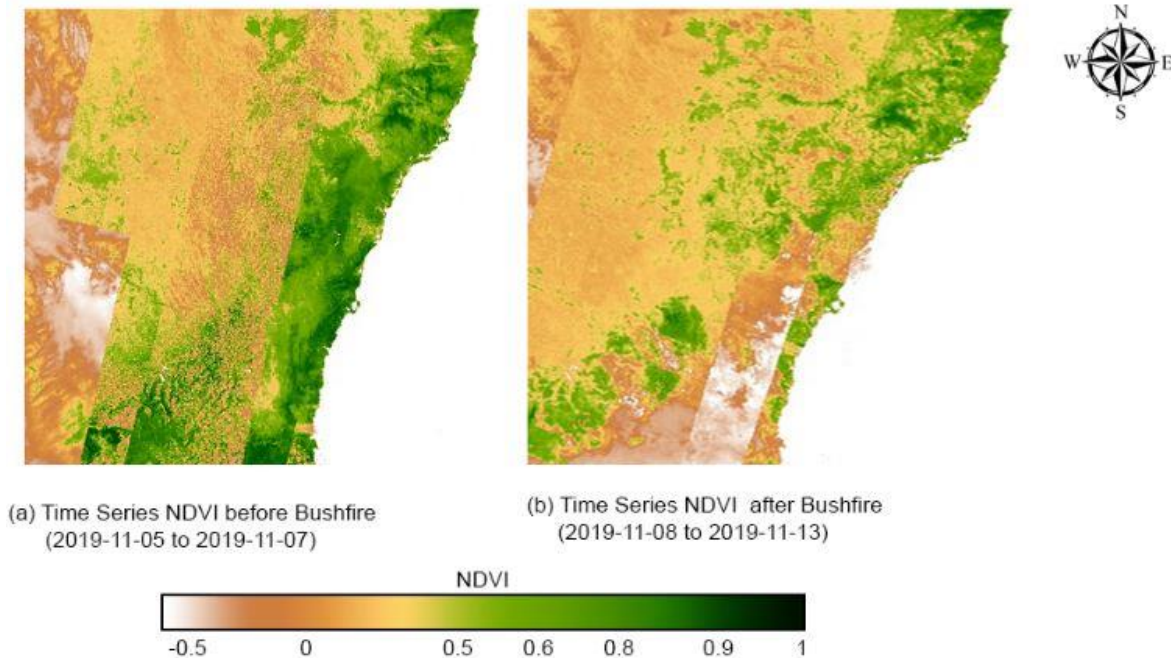


Fig. 3. NDVI of affected cities

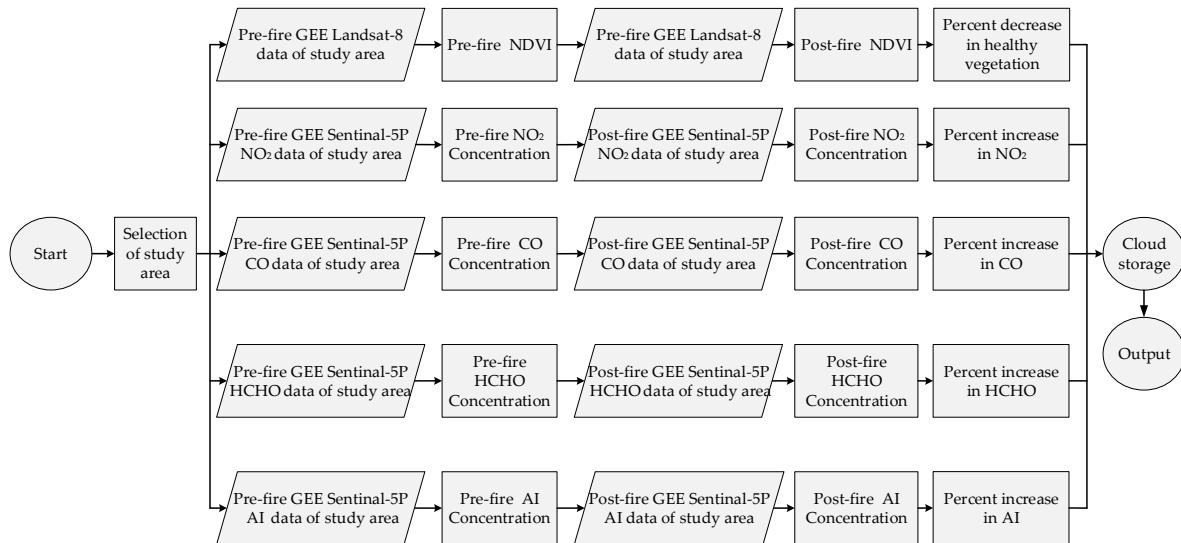


Fig. 4. Proposed strategy

Table 3 post-fire and pre-fire NDVI

S.No	Place	Latitude , Longitude	NDVI Before Fire	NDVI After Fire
1	Mangrove forest	33.3706° S , 151.0568° E	0.6	0.07
2	Acacia Forest	33.7320° S, 150.9084° E	0.3	0.08
3	Kangaroo Valley	34.7342° S, 150.5259° E	0.7	0.45
4	Kangaroo island	35.7752° S, 137.2142°E	0.5	0.35
5	Bairnsdale	37.8333° S, 147.6167° E	0.4	0.20
6	Mallacoota	37.5500° S, 149.7500° E	0.7	0.29
7	Goongerah	37.3500° S, 148.7000° E	0.2	0.03
8	Batemans	35.7119° S, 150.1732° E	0.6	0.12
9	Araluen	35.6218° S, 149.8115° E	0.5	0.23
10	Blue mountains	33.4100° S, 150.3037° E	0.3	0.60
11	Sydney	33.8688° S, 151.2093° E	0.5	0.07
12	Wollemi	33.0174° S, 150.3765° E	0.6	0.11
13	Port Macquarie	31.4333° S, 152.9000° E	0.4	0.14

NDVI calculation gives a result in the range of +1 to -1. As NDVI reaches +1 it indicates temperate and tropical forests, middle values like 0.6 to 0.3 represents detection of meadows and shrubs, values in range of 0.1 or less represents empty areas of rocks, sand or snow, values closer to zero indicates bare soil and rocks and negative values shows detection of clouds, water and snow[27].

Pre and post-fire NDVI analysis presented in **Error! Reference source not found.** identifies that Plenty of healthy vegetation were damaged due to drastic fire. The focus of our work is to investigate impact of wildfire on vegetation in all damaged places of Australia in the first 8 days after fire. Table 3 lists some of most affected places due to wildfire and there

pre and post-fire NDVI. shows the percent decrease in healthy vegetation of affected cities. According to our analysis, the severe decrease in healthy vegetation is noticed for Blue Mountains, in which almost 100% decrease in healthy vegetation has occurred. Which shows extensive damage to vegetation in Blue Mountains forests. Similarly, almost same decrease (88% to 80%) in healthy vegetation are detected for Mangrove forest, Sydney, Goongerah, Wollemi and Batemans. Almost 50% decrease is detected for Araluen and Bairnsdale. The lowest damages are 35.7% and 30% for Kangaroo Valley and Kangaroo island, respectively.

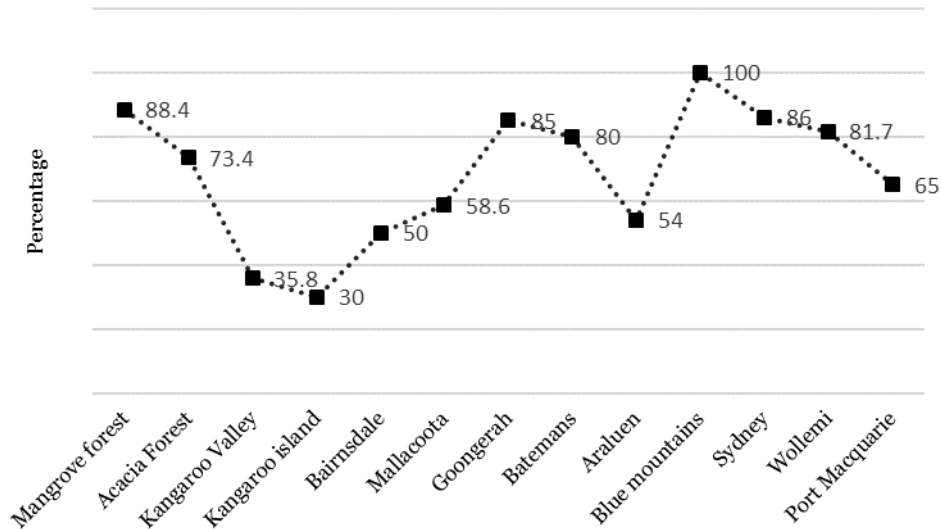


Fig. 5. Percent Decrease in Healthy vegetation

3.2. IMPACT OF FOREST WILDFIRE ON AATMOSPHERIC POLLUTANTS

One of the key features of our proposed satellite-based CPS is pollution monitoring, while utilizing remotely sensed Sentinel-5P data. Figure 6 shows that due to 2019-20 wild fire the smoke created hazardous air quality in NSW and its near cities. In our proposed satellite-based CPS, we investigated the concentration variations of atmospheric gases while employing GEE for processing of remotely sensed Sentinel-5P data.



Fig. 6. Smoke over affected cities using Landsat 8

3.2.1 NITROGEN DIOXIDE (NO₂)

A pollutant, which can severely affect the health of living beings is nitrogen dioxide NO₂ [28]. NO₂ is red-brown acidic gas[29]. Previous studies claimed that exposure of NO₂ to crops can alter their growth rate and may increase the growth rate of fungal pathogens and herbivorous insects [30]. Among many sources of NO₂, the prime sources of NO₂ are natural lightening, soil emissions, biomass fuel burning, industrial burning processes and crop residue burning [31]. According to environmental specialists the climatic conditions variability is mostly linked with NO₂ [32]. In Australia about 80% of NO₂ is produced due to anthropogenic activities like burning of fossil fuels: coal, oil and gas in motor vehicles and power stations [33]. Figure 7 shows NO₂ variations in Australia troposphere during 5th November 2019 to 13th November 2019. **Error! Reference source not found.**(a) shows average NO₂ over affected cities before wild fire. The existence of NO₂ in Figure 8(a) are due to anthropogenic activities in NSW, which is most populated city of Australia. In Figure 8(b), a drastic increase is shown in only 6 days, which shows the effect of heavy wildfire in NSW.

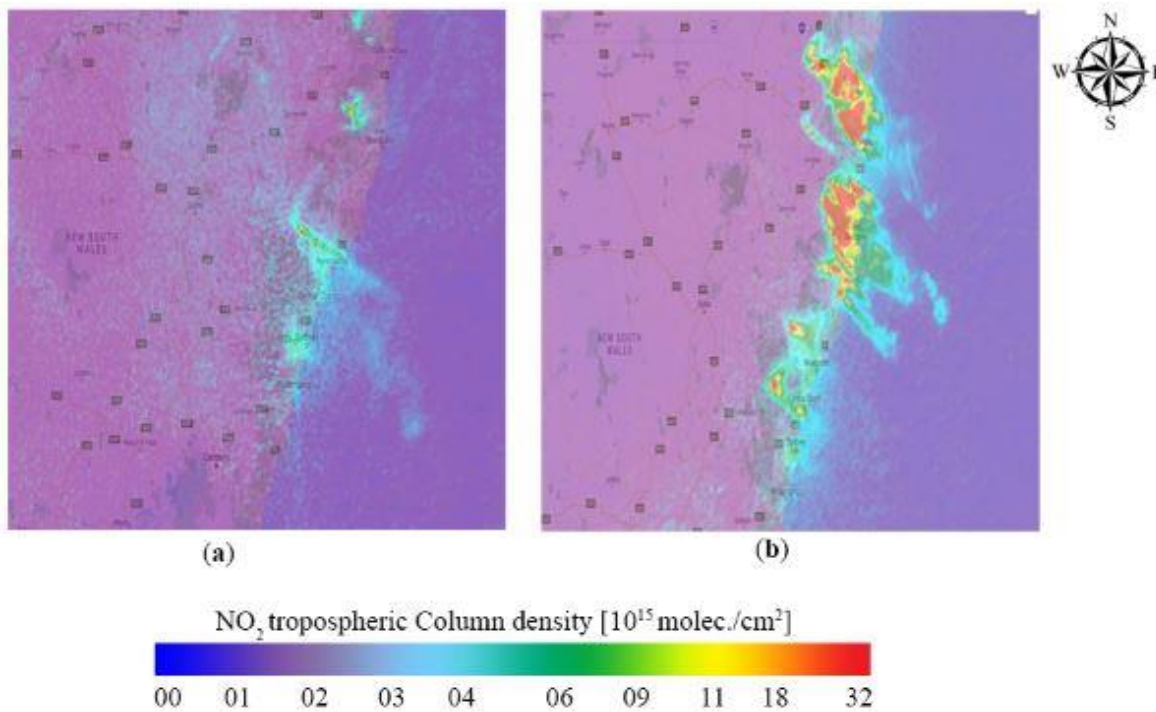


Fig. 7. Averaged during 2019-11-05 to 2019-11-13; (a) Average before Wildfire (2019-11-05 to 2019-11-07); (b) Average after Wildfire (2019-11-08 to 2019-11-13)

Figure 7 shows pre and post-fire NO_2 concentration over affected cities. Our analysis estimated pre-fire and post-fire averaged NO_2 is $8.3 \times 10^{15} \text{ molec./cm}^2$ and $17.6 \times 10^{15} \text{ molec./cm}^2$, respectively. It can be observed from Figure 8 that the highest increase in the concentration of

NO_2 is 275% over Mocksville, which shows most polluted environment during these days and the lowest increase in the concentration of NO_2 is 4.3% is detected in the troposphere of Sydney. The average increase in NO_2 during 5th November to 13th November is 112%.

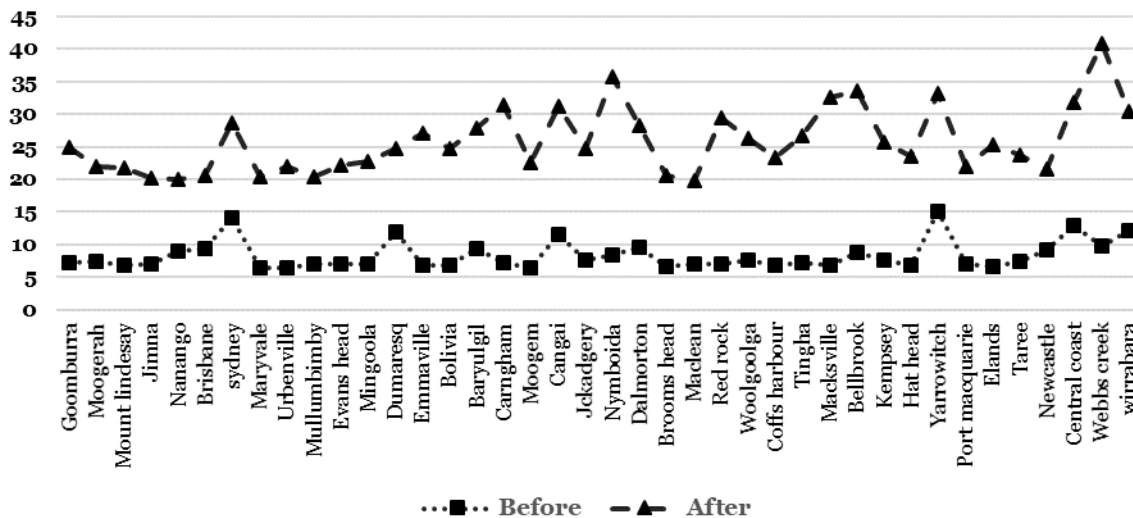


Fig. 8. Pre-fire and post-fire NO_2 concentration ($10^{15} \text{ molec./cm}^2$)

Figure 1 Pre-fire and post-fire NO_2 concentration ($10^{15} \text{ molec./cm}^2$)

3.2.2. CARBON MONOXIDE (CO)

Biomass burning is major source of Carbon Monoxide (CO) in troposphere [34]. In Australia and in many other countries CO is the 6th major air pollutant. Excess of CO in troposphere is poisonous to humans and as it is tasteless and odorless so it cannot be detected by humans. Increased level of CO is also reducing hemoglobin in red blood cells. Although, CO is not

source of climate change directly but its abundance can drastically increase greenhouse gases like methane (CH_4) and carbon dioxide (CO_2). Concentration of CO can provide information of anthropogenic activities because it is found as a useful tracer of biomass burning and anthropogenic pollutions [35, 36].

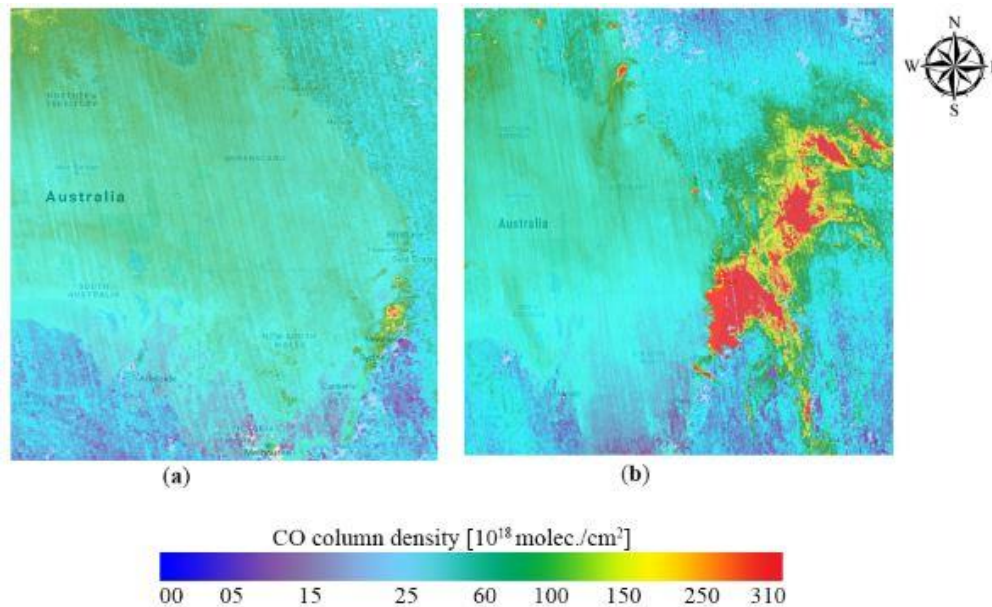


Fig. 9. Averaged CO during 2019-11-05 to 2019-11-13: (a) Average CO before Wildfire (2019-11-05 to 2019-11-07); (b) Average CO after Wildfire (2019-11-08 to 2019-11-13)

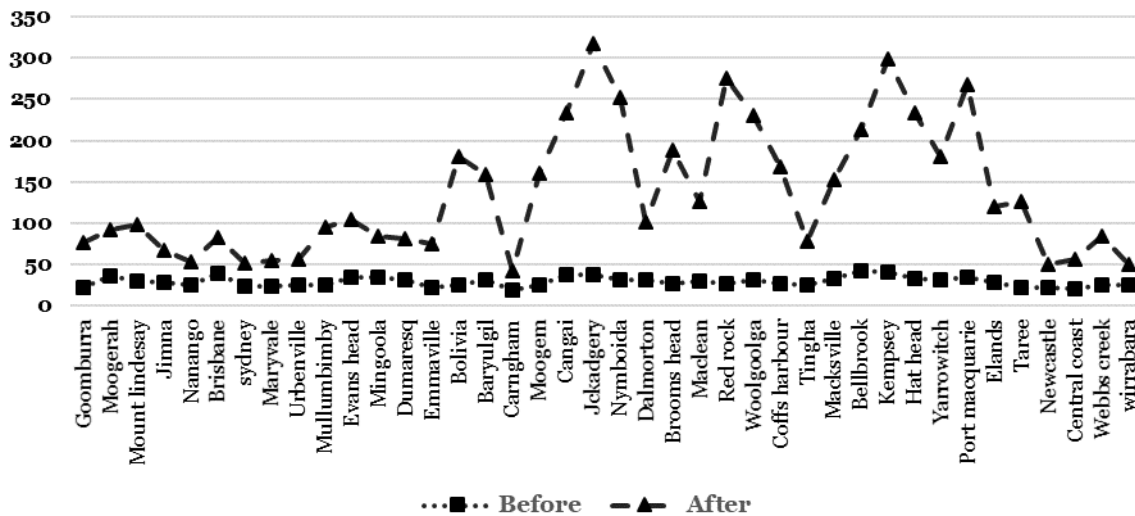


Fig. 10. Pre-fire and post-fire CO concentration()

Using our proposed satellite-based CPS the variation in the level of CO due to forest wildfire is investigated. Error! Reference source not found. shows average concentration of CO in Australian troposphere during 5th November 2019 to 13th November 2019. Error! Reference source not found. (a) shows average CO over affected cities before bush fire. Error! Reference source not found. (a) clearly shows that before the incident of forest wildfire, most places in Australia have not hazardous level of CO. Only few cities like NSW and its nearby cities have a little bit excess of CO in its air. The reason of existence of CO before forest wildfire is anthropogenic activities in these

3.2.3. AEROSOL INDEX (AI)

Aerosol Index (AI) is a qualitative measure of the presence

most populated and industrial cities of Australia. Our analysis estimated pre-fire averaged CO as $29.4 \times 10^{18} \text{ molec./cm}^2$. While Error! Reference source not found. (b) shows an alarming increase in 6 days due to forest wildfire. Post-fire Averaged CO is measured $106.2 \times 10^{18} \text{ molec./cm}^2$, Which is 260% increase as compared to pre-fire CO. Error! Reference source not found. shows pre and post fire CO concentration over affected cities. The tremendous increase detected is 818.2% over Red Rock and the lowest increase is detected in troposphere of Nanango, which is 3.8%.

of UV-absorbing aerosols, such as mineral dust and smoke [37]. The Aerosol Index (AI) product has been widely used in

different applications including monitoring of the sources and sinks of carbonaceous aerosols from biomass burning and wild fires, dust storms from deserts, and volcanic ash. AI in troposphere can be exceeded by anthropogenic activities like burning of agricultural residue and fireworks [37]. Using our proposed satellite-based CPS the variation in the concentration level of AI due to forest wildfire is

investigated. Figure 13=2 shows Averaged concentration of AI in Australia troposphere during 5th November 2019 to 13th November 2019. Figure 13(a) shows average AI over affected cities before bush fire, which is measured as $-10.9 \times 10^{19} molec./cm^2$.

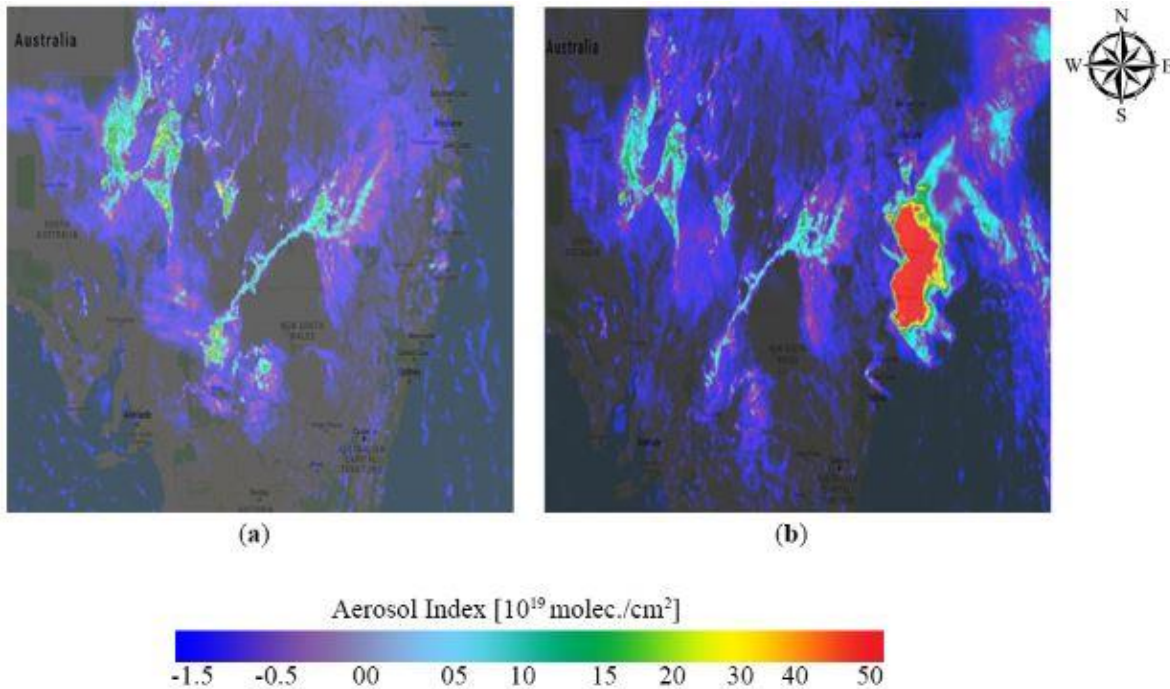


Fig. 11. Averaged AI during 2019-11-05 to 2019-11-13; (a) Average Aerosol Index before Wildfire (2019-11-05 to 2019-11-07) ;(b) Average Aerosol Index after Wildfire (2019-11-08 to 2019-11-13)

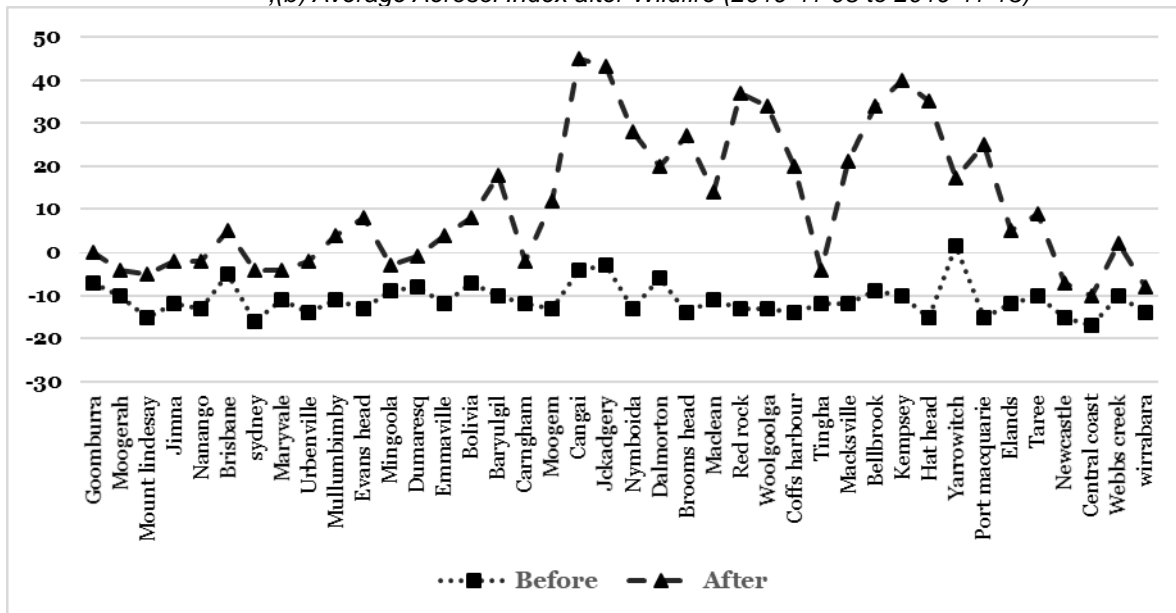


Fig. 12. Pre-fire and post-fire AI concentration ()

In Error! Reference source not found.(b), drastic increase of $17.9 \times 10^{19} molec./cm^2$ in the average concentration level of AI is observed in 6 days period, which shows the effect of heavy wildfire in NSW. Error! Reference source not found. shows pre and post fire AI concentration over affected cities. From Error! Reference source not found., it is observed that the highest increase of 1633% is observed over

Jekadgery and the lowest increase is detected in troposphere of Carringham, which is 16%. Overall increase in AI during 5th November to 13th November is 264%.

3.2.4. Formaldehyde (HCHO)

Formaldehyde (HCHO) is found one of carcinogen in among 187 hazardous air pollutants [38]. HCHO does not persist for

long but it is toxic. Main sources of **HCHO** in Australia is anthropogenic activities like industrial emissions and fuel combustion from traffic and biomass combustion (forest fire) or decompositions of volcanoes. But the major source of **HCHO** in Australia is forest fire as burning of biomasses contribute to HCHO in troposphere. Using our proposed satellite-based cyber-physical system the variation in the concentration level of **HCHO** due to forest wildfire is investigated. Averaged **HCHO** concentration in Australia troposphere during pre and post-fire scenario is shown in Figure 14(a) shows pre-fire **HCHO** over Australia. It is observed that during pre-fire normal

days scenario, averaged **HCHO** concentration of $15.6 \times 10^{15} \text{ molec./cm}^2$ is detected by our proposed satellite-based cyber-physical system. Similarly, using satellite-based CPS, while utilizing post-fire remotely sensed data for the period 2019-11-08 to 2019-11-13, shows an excess averaged **HCHO** concentration value of $37.9 \times 10^{15} \text{ molec./cm}^2$. Furthermore, it is observed that the highest increase in the concentration of **HCHO** is 1750% over Urbenville and the lowest increase is detected in troposphere of Moogerah which is 7.2%. The overall tremendous increase of 144% is due to heavy forest fire.

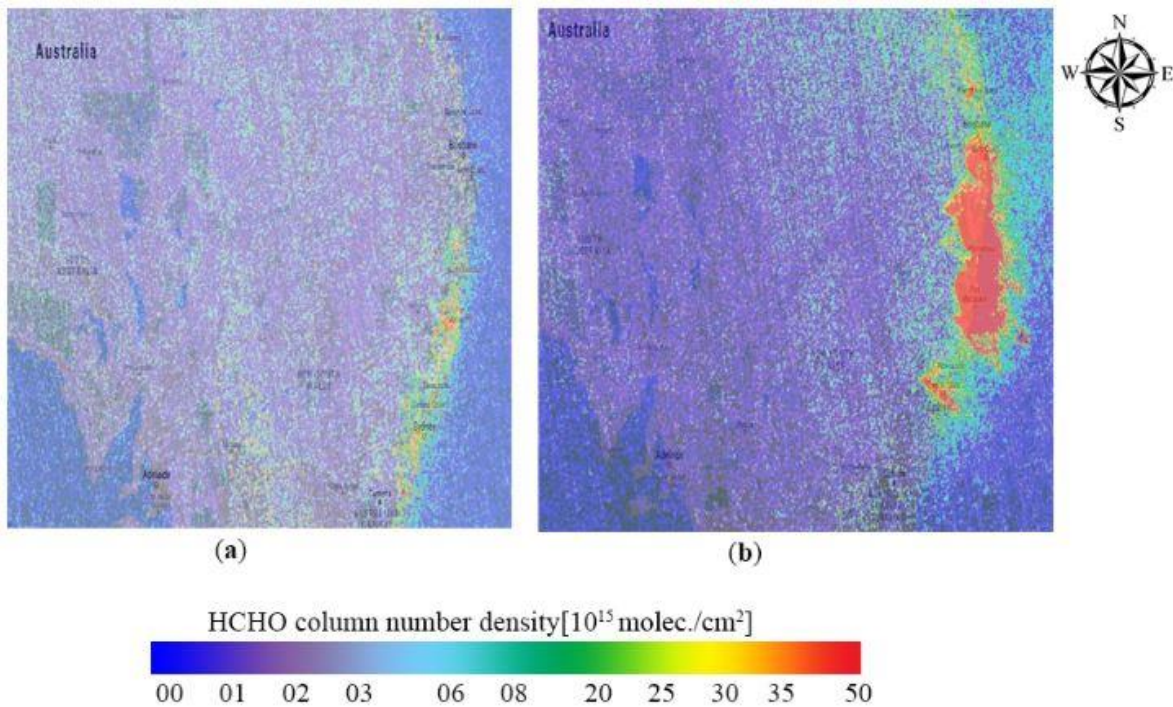


Fig. 13. Averaged HCHO during 2019-11-05 to 2019-11-13; (a) Average HCHO before Wildfire (2019-11-05 to 2019-11-07) ;(b) Average HCHO after Wildfire (2019-11-08 to 2019-11-13)

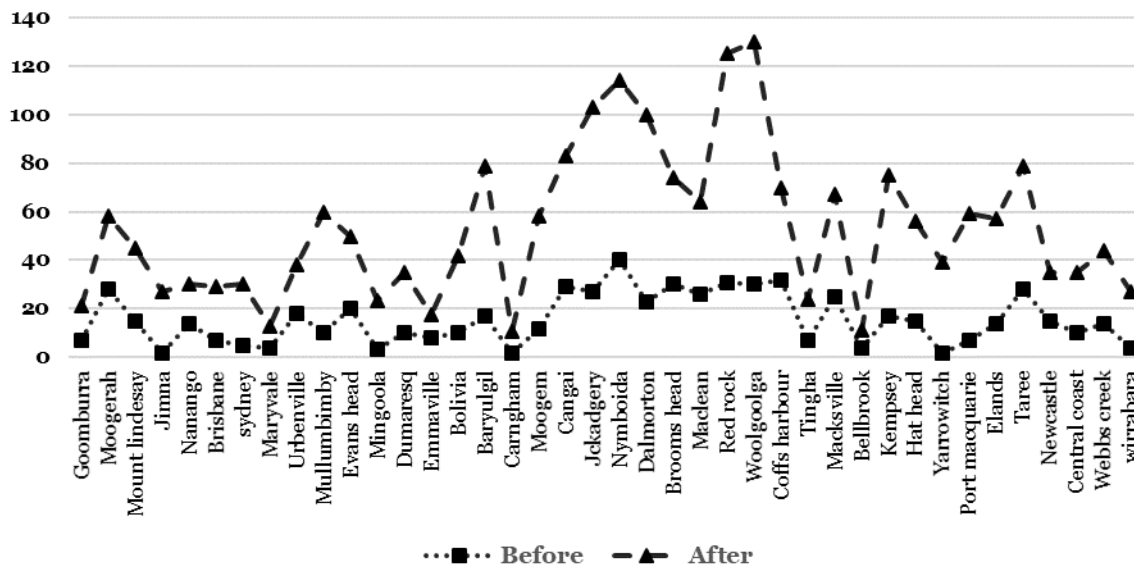


Fig. 14. Pre-fire and post-fire HCHO concentration

4.CONCLUSION

In this paper we proposed a cyber-physical based forest monitoring system(CPS). CPS uses Landsat 8 and Sentinel-

5P data to detect damages in healthy vegetation and environment respectively. Sentinel-5P is found capable of sensing all atmospheric gasses while Landsat 8 is used for calculating NDVI. 2019-20 forest fire was ignited from NSW region on 8th November 2019. Pre-fire dataset of Landsat 8, from 5th to 7th November of 2019, was processed in CPS to compute pre-fire NDVI. Post-fire NDVI was computed by using 8th to 13th November Landsat 8 dataset in CPS. Thirteen (13) places were found mostly vegetation affected with 100% decrease in healthy vegetation over Blue Mountains and lowest decrease of 30.3% for Kangaroo island. As burning of forest emits gases like **NO₂**, **CO**, **HCHO** and Aerosol Index(AI). Along with damage to vegetation this work also estimated drastic increase in tropospheric **NO₂**, **CO**, **HCHO** and AI. Among many other satellites Sentinel-5p is capable of detecting all these gasses. Pre-fire dataset of **NO₂**, from 5th to 7th November of 2019, was processed in CPS to compute pre-fire averaged **NO₂** concentration of $8.3 \times 10^{15} \text{ molec./cm}^2$. Post-fire averaged **NO₂** concentration of $17.6 \times 10^{15} \text{ molec./cm}^2$ was computed using 8th to 13th November Sentinel-5P dataset in CPS. A tremendous increase of 112% is estimated from 5th to 13th November with 40 cities **NO₂** concentration as shown in Figure 14. Pre-fire dataset (5th to 7th November) of **CO**, **AI** and **HCHO** are processed in CPS. An increase of 260%, 264% and 144% are estimated for **CO**, **AI** and **HCHO** concentration in Australia troposphere after wild fire. This drastic increases detection in tropospheric gases proved that as compared to up-to-date fire monitoring systems, our proposed CPS have a great potential in providing efficient and accurate results.

ACKNOWLEDGMENT

The authors wish to thank A, B, C. This work was supported in part by a grant from XYZ.

REFERENCES

- [1] BBC, Australia bushfires. 2019: <https://www.bbc.com/>.
- [2] EOS, Five Environmental Consequences of Australia's Fires 2020.
- [3] Accuweather, Australia wildfire damages and losses to exceed \$100 billion, AccuWeather estimates 2020.
- [4] Erten, E., V. Kurgun, and N. Musaoglu. Forest fire risk zone mapping from satellite imagery and GIS: a case study. in XXth Congress of the International Society for Photogrammetry and Remote Sensing, Istanbul, Turkey. 2004.
- [5] Wu, F.-J., Y.-F. Kao, and Y.-C. Tseng, From wireless sensor networks towards cyber physical systems. *Pervasive and Mobile computing*, 2011. 7(4): p. 397-413.
- [6] Lee, I. Sokolsky, O., "Health Cyber Physical Systems," in 47th ACM/IEEE Design Automation Conference, Anaheim. 2010.
- [7] Liu, Z., et al., Cyber-physical-social systems for command and control. *IEEE Intelligent Systems*, 2011. 26(4): p. 92-96.
- [8] Muratov, Y.R., et al. Estimation of distance to objects by stereovision. in 2015 4th Mediterranean Conference on Embedded Computing (MECO). 2015. IEEE.
- [9] Hoang, D.D., H.-Y. Paik, and C.-K. Kim, Service-oriented middleware architectures for cyber-physical systems. *International Journal of Computer Science and Network Security*, 2012. 12(1): p. 79-87.
- [10] Józwiak, L., Embedded computing technology for highly-demanding cyber-physical systems. *IFAC-PapersOnLine*, 2015. 48(4): p. 19-30.
- [11] Birdal, A.C., U. Avdan, and T. Türk, Estimating tree heights with images from an unmanned aerial vehicle. *Geomatics, Natural Hazards and Risk*, 2017. 8(2): p. 1144-1156.
- [12] Guangmeng, G. and Z. Mei, Using MODIS land surface temperature to evaluate forest fire risk of northeast China. *IEEE Geoscience and Remote sensing letters*, 2004. 1(2): p. 98-100.
- [13] Sivrikaya, F., et al., Evaluation of forest fire risk with GIS. *Polish Journal of Environmental Studies*, 2014. 23(1).
- [14] Teodoro, A.C. and L. Duarte, Forest fire risk maps: a GIS open source application—a case study in Norwest of Portugal. *International Journal of Geographical Information Science*, 2013. 27(4): p. 699-720.
- [15] Çolak, E. and F. Sunar, Evaluation of forest fire risk in the Mediterranean Turkish forests: A case study of Menderes region, Izmir. *International Journal of Disaster Risk Reduction*, 2020: p. 101479.
- [16] Saglam, B., et al., Spatio-temporal analysis of forest fire risk and danger using LANDSAT imagery. *Sensors*, 2008. 8(6): p. 3970-3987.
- [17] García-Llamas, P., et al., Environmental drivers of fire severity in extreme fire events that affect Mediterranean pine forest ecosystems. *Forest ecology and management*, 2019. 433: p. 24-32.
- [18] Ahmadi, V., Crisis Management in Forest Fire by use of Image Landsat in Model Fire Risk (Case Study: Bioreh Protected Area, Illam Province). *Geospatial Engineering Journal*, 2019. 10(2): p. 27-37.
- [19] Akbulak, C., et al., Forest fire risk analysis via integration of GIS, RS and AHP: The Case of Çanakkale, Turkey. *Journal of Human Sciences*, 2018. 15(4): p. 2127-2143.
- [20] Theys, N., et al., Global monitoring of volcanic SO₂ degassing with unprecedented resolution from TROPOMI onboard Sentinel-5 Precursor. *Scientific reports*, 2019. 9(1): p. 2643.
- [21] Ingmann, P., et al., Requirements for the GMES Atmosphere Service and ESA's implementation concept: Sentinels-4/-5 and-5p. *Remote Sensing of Environment*, 2012. 120: p. 58-69.
- [22] Shen, L., et al., An evaluation of the ability of the Ozone Monitoring Instrument (OMI) to observe boundary layer ozone pollution across China: application to 2005–2017 ozone trends. *Atmospheric Chemistry and Physics*, 2019. 19(9): p. 6551-6560.
- [23] Goldberg, D.L., et al., Enhanced capabilities of TROPOMI NO₂: Estimating NO_x from North American cities and power plants. *Environmental science & technology*, 2019.
- [24] Gorelick, N., et al., Google Earth Engine: Planetary-scale geospatial analysis for everyone. *Remote Sensing of Environment*, 2017. 202: p. 18-27.
- [25] Landgrebe, D.A. Some fundamentals and methods for hyperspectral image data analysis. in *Systems and technologies for clinical diagnostics and drug discovery II*. 1999. International Society for Optics and Photonics.
- [26] Kutnjak, H., et al., Seasonal phenology dynamics of alfalfa consociation with Italian ryegrass based on NDVI from Sentinel-2. *sa55*, 2020: p. 49.
- [27] hub, S. NDVI (Normalized Difference Vegetation Index). 2005; Available from: <https://www.sentinel-hub.com/eoproducts/ndvi-normalized-difference->

[vegetation-index.](#)

- [28] Hvidtfeldt, U.A., et al., Long-term residential exposure to PM_{2.5}, PM₁₀, black carbon, NO₂, and ozone and mortality in a Danish cohort. *Environment international*, 2019. 123: p. 265-272.
- [29] Abbasi, A. and J.J. Sardroodi, TiO₂/graphene oxide heterostructures for gas-sensing: Interaction of nitrogen dioxide with the pristine and nitrogen modified nanostructures investigated by DFT. *Surface Review and Letters*, 2019. 26(04): p. 1850170.
- [30] Shon, Z.-H., K.-H. Kim, and S.-K. Song, Long-term trend in NO₂ and NO_x levels and their emission ratio in relation to road traffic activities in East Asia. *Atmospheric environment*, 2011. 45(18): p. 3120-3131.
- [31] Richter, A., et al., GOME measurements of stratospheric and tropospheric BrO. *Advances in Space Research*, 2002. 29(11): p. 1667-1672.
- [32] Zheng, Z., et al., Spatial Variation of NO₂ and Its Impact Factors in China: An Application of Sentinel-5P Products. *Remote Sensing*, 2019. 11(16): p. 1939.
- [33] Heritage, D.o.t.E.a., Air quality fact sheet. 2005.
- [34] Qu, P. and Y. Yin. Impacts of Summer Biomass Burning in Australia on Carbon Monoxide, Ozone and Aerosols in the Troposphere of Darwin. in 2008 International Workshop on Education Technology and Training & 2008 International Workshop on Geoscience and Remote Sensing. 2008. IEEE.
- [35] Edwards, D., et al., Satellite- observed pollution from Southern Hemisphere biomass burning. *Journal of Geophysical Research: Atmospheres*, 2006. 111(D14).
- [36] Yurganov, L., et al., Satellite-and ground-based CO total column observations over 2010 Russian fires: accuracy of top-down estimates based on thermal IR satellite data. UMBC Physics Department, 2011.
- [37] Badarinath, K., et al., Analysis of aerosol and carbon monoxide characteristics over Arabian Sea during crop residue burning period in the Indo-Gangetic Plains using multi-satellite remote sensing datasets. *Journal of Atmospheric and Solar-Terrestrial Physics*, 2009. 71(12): p. 1267-1276.
- [38] Zhu, L., et al., Formaldehyde (HCHO) as a hazardous air pollutant: Mapping surface air concentrations from satellite and inferring cancer risks in the United States. *Environmental science & technology*, 2017. 51(10): p. 5650-5657.